

General Disclaimer

One or more of the Following Statements may affect this Document

- This document has been reproduced from the best copy furnished by the organizational source. It is being released in the interest of making available as much information as possible.
- This document may contain data, which exceeds the sheet parameters. It was furnished in this condition by the organizational source and is the best copy available.
- This document may contain tone-on-tone or color graphs, charts and/or pictures, which have been reproduced in black and white.
- This document is paginated as submitted by the original source.
- Portions of this document are not fully legible due to the historical nature of some of the material. However, it is the best reproduction available from the original submission.

(NASA-TM-85148) ANALYSES OF THE KONUS
CATALOGUE OF GAMMA-RAY BURSTS WITH THE
THERMAL SYNCHROTRON MODEL (NASA) 47 P
HC A03/MF A01

N83-14058

CSCL 03B

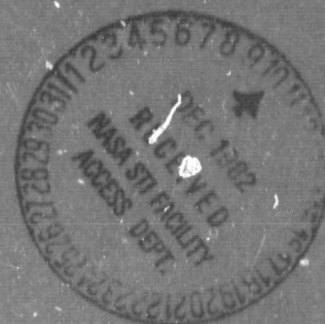
Unclass

G3/93 02113

ANALYSES OF THE KONUS CATALOGUE OF GAMMA-RAY BURSTS WITH THE THERMAL SYNCHROTRON MODEL

by

E.P. Liang, T. Jernigan and R. Rodrigues



NATIONAL AERONAUTICS AND SPACE ADMINISTRATION
Grant NGR 05-020-038

SUIPR Report No. 943

September 1982



INSTITUTE FOR PLASMA RESEARCH
STANFORD UNIVERSITY, STANFORD, CALIFORNIA

ANALYSES OF THE KONUS CATALOGUE OF
GAMMA-RAY BURSTS WITH THE
THERMAL SYNCHROTRON MODEL

E. P. Liang

Lawrence Livermore National Laboratory,⁺ University of California
and Institute for Plasma Research,^{*} Stanford University

and

T. Jernigan

Ames Research Center, NASA
and Space Science Program, Stanford University

and

R. Rodrigues

Stanford University

⁺Operated under DOE contract W-7405-Eng-48

^{*}Partially supported by NASA Grant NGR 05-020-668

Submitted to Ap. J.

Abstract

We analyze the approximately 150 reported gamma burst spectra of the Konus catalogue (Mazets et al. 1981) using the thermal synchrotron model. An overwhelming majority of these spectra can be satisfactorily fitted by theoretical thermal synchrotron spectra of mildly relativistic electrons in strong magnetic fields, making the strong-field neutron star picture at least self-consistent. Valuable additional information is also extracted from various spectral features contained in many of the events.

I. INTRODUCTION

In a recent article we pointed out that many of the observed gamma-ray burst spectra can be fitted by optically thin thermal synchrotron (or high-harmonic cyclotron, hereafter abbreviated TS) emission of mildly relativistic ($kT_e \sim mc^2$) electrons (Liang 1982). In most cases the TS fits are at least as satisfactory as the conventionally adopted thermal bremsstrahlung (TB) or free-free spectra. The success of the TS fits corroborates the picture of strongly magnetized neutron stars as gamma-burst sources. Since then we have performed a detailed and systematic analysis of the entire Konus Catalogue (Mazets et al. 1981) containing spectral data of ~ 120 separate events and 150 burst spectra (20-1500 keV) obtained by the Konus experiments from 1978 through 1980. This article summarizes the major findings. Some of these results have far-reaching implications for future model building of the gamma-burst sources.

Despite the controversy surrounding the alleged emission and absorption features reported by Mazets et al. (1981) in many of the events (due to uncertainties introduced by the deconvolution procedure [Fenimore et al. 1982c]), we believe that the overall continuum shapes of the spectral data remain trustworthy, since similar continua are also observed by other groups (e.g., Cline et al. 1975, Gilman et al. 1980). But it remains interesting for the experimentalist to try to deconvolve Mazets' data with an assumed TS instead of TB spectrum to see if there are significant differences.

II. SPECTRAL FITS

Using the analytic formula derived by Petrosian (1981) which is valid in the regime $\nu \gg \nu_L/T$ ($\nu_L \equiv eB/2\pi mc$ is the Larmor frequency and $T \equiv kT_e/mc^2$; see also Trubnikov 1961, Lamb and Masters 1979), we attempt to fit all 150 spectra of Mazets' catalogue with the TS model. Since chi-square analyses of the entire collection is prohibitively labor consuming, we simply used variable-endpoint fitting and eyeball inspections for the goodness of the fit. Overall, we are convinced that over 80 percent of the fits should be considered satisfactory. The remaining spectra either have very poor statistics or have shapes clearly distinct from the monotonic convex shapes of TS (or TB) spectra. These anomalous spectra, however, may still be produced by cyclo-synchrotron emission of nonthermal electrons, or they could simply be the composite of time-varying spectra due to changing electron distributions within the ~ 4 sec integration period. In fact, considering the ultra-short cooling time of the electrons ($t_{\text{cooling}} \ll t_{\text{Coulomb relax}}$, independent of whether the cooling is due to TS, TB or inverse Compton (IC) as proposed by Fenimore et al. [1982a]), it is just remarkable that most sources can maintain close to thermal distributions at all. Collective plasma processes must be extremely efficient in thermalizing the electrons, a clue to be noted by all model builders of gamma-ray bursts.

Even among the "good" fits, there are systematic trends of small deviations from the TS continuum shape. Some of the more significant ones are listed here. (1) Many of the spectra

deviate from the TS fit at the high-energy tail (mostly dropping below). This may be due to systematic error (e.g., detector deficiency near detection limit). If it is intrinsic, it would suggest that the high-energy-tail electrons often fail to stay Maxwellian, an expected phenomenon since they have the fastest cooling and slowest relaxation rates. A few of the spectra with high-energy excess may also be due to self-Comptonization (Liang 1981). (2) Some spectra have apparent excess emission in mid-energies (100-500 keV). If they are real, it could be due to broadened emission lines (e.g., redshifted 511 keV line or cyclotron line with $B \geq 10^{13}$ G) or Comptonization. (3) Some spectra show low-energy cutoff. These would most likely be due to self-absorption. (4) A number of spectra show conspicuous excess emission at the low-energy end. In the TS picture, it would be most natural to attribute them to low-energy harmonic emissions (cyclotron lines). Several spectra, in fact, show double peaks characteristic of the first and second harmonics (Sec. V). The undisputed detection of the first few harmonics would be the strongest evidence for the TS model. (5) Some spectra have "absorption" dips in the 30-70 keV range, but the continuum continues to rise below the frequency of the dip. The reality of these absorption features has been challenged by some (Fenimore et al. 1982c, 1982b). Even if they are real, their interpretation is by no means obvious, since the rise of the continuum below the dip energy might suggest that the field strength responsible for the TS continuum is weaker than the absorption region. One way out is that since the TS continuum

emission region is much hotter than the line absorption region (as evidenced by the narrowness of some of the lines), the first harmonic emission peak would be Doppler shifted down ($\nu_L^0 = \nu_L / (1 + c_v T) c_v \approx 2-3$) to undetectable energies, while the absorption feature would stay near the unshifted value ν_L .

Figures 1-6 provide samples of TS fits to the data and representatives of the above five categories of deviants.

III. DISTRIBUTION OF ν_c

The spectral fitting uniquely determines the "critical frequency" $\nu_c = \nu_L T^2 \langle \sin \theta \rangle$, where θ is the angle between magnetic field lines and the line of sight. In Figure 7a we plot the histogram for the distribution of ν_c for all the ~ 150 spectra. A more meaningful histogram is the distribution of ν_c in terms of events (~ 120), where we pick only the highest ν_c for each event with reported spectral evolution. It is clear that the distribution peaks between 2-5 keV and cuts off sharply at ~ 12 keV. If we assume a universal field strength of $B \langle \sin \theta \rangle = 2 \times 10^{12}$ G ($\nu_L \langle \sin \theta \rangle = 23$ keV, clearly not true in some cases), then the temperature distribution peaks between .2-.7 mc^2 (top scales of Fig. 6). It is significant that few events have $T \geq mc^2$ (unless $B \langle \sin \theta \rangle$ was $\ll 10^{12}$ gauss).

IV. TIME EVOLUTIONS

Mazets' catalogue included data on the spectral time-evolution for about 15 of the events. In Figure 8 we plot the time development of ν_c for 14 of these events (the other one has a late-time spectrum deviating so badly from TS that no meaningful ν_c could be determined). They show a distinct trend of initial exponential decay (with decay constant \sim sec) but leveling or even bouncing back after a couple of e-foldings. This should be a useful clue to modeling the energy source. Two of the events also show evidence of early-time self-absorption and late-time harmonic emissions. We will discuss the important implications of such features for these two events in a separate article (Liang 1983). Table I tabulates the crudely estimated decay constants for ν_c of all events.

V. SPECTRA WITH HARMONIC FEATURES

Taken at face value, ~ 24 of Mazets' spectra show discernible low-energy features (in excess of the TS continuum), interpretable as first harmonic emission. These spectra allow us to determine B and T separately (Table II). It is interesting to note that, overall, the ones with observable harmonics tend to have higher v_c than the overall norm. Eight of these events also exhibit possible second harmonic peaks (at $\sim 2v_1$). The ratio of the first to second peak, as well as upper bounds to the line width are also consistent with the theoretically predicted values, except for the event of 5-24-79 (see Table III). In Figure 9 we plot the histograms for the T and B distributions. It is remarkable how narrow the distributions are. We believe the existence of harmonic features is the strongest evidence in favor of the TS model.

VI. SPECTRA EXHIBITING SELF-ABSORPTION

Approximately a dozen events contain spectra with low-energy cutoff interpretable as self-absorption. For these spectra we can determine $n_e h$ (electron column density)/ TK_2 (T^{-1}) (K_2 Bessel function, cf. Eq. 13, Liang 1982). If, moreover, we assume that ν_L^0 lies at or below the peak, then lower bounds to T , $n_e h$, L_{syn}/A (synchrotron luminosity per unit emission area, the coefficients in Eqs. (11), (14), etc., of Liang 1982 should be lowered by a factor of ~ 3) and d (source distance)/ $A^{1/2}$ can be estimated. Table IV lists these values. Despite the uncertainties in the distance estimates, some of these events are evidently extragalactic (unless A is tiny), showing that the 3-5-79 event is not unique (Ramaty et al. 1981, Liang 1981). We must emphasize, however, that these few sources likely represent the most distant ones, since all others do not show self-absorption down to 15-30 keV. Hence the TS interpretation is consistent with other evidence showing that the vast majority of gamma-burst sources are galactic. Also, since TK_2 likely lies in the range 0.5-0.05, the electron column densities are uniformly around 10^{21} - 10^{22} cm^{-2} . These are remarkably optically thin sources.

VII. COMPARISON BETWEEN TS, TB AND IC SPECTRAL FITS

For a spectral fit that is geared towards the mid-energy data points (50-500 keV), the three theoretical spectra, namely, TS, TB and IC should in principle be distinguishable at the low- and high-energy ends. Unfortunately, most spectra do not have enough data points at the extremes to distinguish clearly among the three models. Moreover, low-energy absorption and high-energy non-thermal emissions may also mask the underlying thermal spectra. Figure 8 represents one of those "clean" thermal spectra with a monotonic curvature extending over the widest observed energy range (20-1500 keV). Plotted on it are three best-fit theoretical spectra corresponding to TS, TB and IC. It is clear that TS and TB are almost indistinguishable except at the highest energy, where the data are poor. On the other hand, IC is not so good a fit overall despite its three free parameters (compared with two for the others). The high n_{eh} required by the IC fit and the high n_{eh}^2 of the TB fit would make them incompatible with the strong-field neutron star picture (Table V).

VIII. SUMMARY

It is clear that a huge amount of useful information is hidden in the data published by Mazets et al. (1981). We are convinced that an overwhelming majority of these spectra can be satisfactorily interpreted as thermal synchrotron radiation with $\nu_c (= B/(8.62 \times 10^{10} \text{ G}) T^2)$ lying between 1-12 keV, although this interpretation is not unique. This is basically consistent with the picture of hot ($kT \sim mc^2$) thermal emission from strong field ($B \sim 10^{12} \text{ G}$) neutron star surfaces. Various spectral features provide additional valuable information about the source, once we adopt the TS interpretation. In particular, several sources showing self-absorption can be estimated to lie as far as the 3-5-79 event (e.g., the Magellanic clouds), and sources with detectable first harmonics have very narrow distributions in temperature and magnetic field strength.

Clearly, we have only scratched the tip of the iceberg. Future analyses taking into account, e.g., the correlation between spectra and intensity variations, annihilation-line features, etc., promise to provide even more information. It is to be hoped that such information will ultimately suffice to reveal the true nature of the majority of the events, which likely have a rather universal origin. Ruderman's wishes (1975) may yet be fulfilled after all.

REFERENCES

- Cline, T. L. 1975, Ann. N.Y. Acad. Sci., 262 (eds. Bergmann, P., Fenyves, E. and Motz, L.; New York: NYAS), 159.
- Fenimore, E. E. et al. 1982a, Nature, 297, 665.
- Fenimore, E. E. et al. 1982b, LANL preprint, to appear in COSPAR Symp. Proc. (Ottawa, Canada), May 1982.
- Fenimore, E. E., Laros, J. G., Klebesadel, R. W., Stockdale, R. E. and Kane, S. 1982c, AIP Conf. Proc. No. 77 eds. Lingenfelter, R. E., Hudson, H. S. and Worrall, D. M. (New York: AIP), p. 20.
- Gilman, D. Metzger, A. E., Parker, R. H., Evans, L. G., Trombka, J. I. 1980, Ap. J., 236, 951.
- Lamb, D. Q. and Masters, A. R. 1979, Ap. J. (Lett.), 234, L117.
- Lamb, D. Q. 1982, AIP Conf. Proc. No. 77, eds. Lingenfelter, R. E., Hudson, H. S., and Worrall, D. M. (New York: AIP), p. 249.
- Liang, E. P. 1981, Nature, 292, 319.
- Liang, E. P. 1982, Nature (Sept.), to appear.
- Liang, E. P. 1983, submitted to Ap. J. Lett.
- Mazets, E. P., Golenetskii, S. V., Il'inskii, V. N., Panov, V. N., Aptekar, R. L., Gur'yan, Y. A., Proskura, M. P., Sokolov, I. A., Sokolova, Z. Y., Kharitonova, T. V., Dyatchkov, A. V. and Khavenson, N. G. 1981, Ap. and Sp. Sci. 80, 7.
- Petrosian, V. 1981, Ap. J., 251, 727.
- Ramaty, R., Lingenfelter, R. E. and Bussard, R. W. 1981, Ap. and Sp. Sci., 75, 193.

Ruderman, M. '974, Ann. N.Y. Acad. Sci., 262 eds. Bergmann, P.,
Fenyves, E. and Motz, L. (New York: NYAS).
Trubnikov, B. A. 1961, Phys. Fluids, 4, 195.

ORIGINAL PAGE IS
OF POOR QUALITY

Table I. Initial Decay Time of ν_c

Event	$\tau(\pm \Delta t / \Delta \ln \nu_c) / \text{sec}$
9-14-78	6.9
9-18-78	-9.6 \rightarrow +9.1
11-04-78	2.3
11-19-78	5.8
11-24-78	2.4
3-05-79	6.0
3-13-79	5.7
3-25-79	13.2
3-29-79	4.1
4-02-79B	5.9
6-04-79	3.7
10-14-79	2.3
11-09-79	3.2
11-11-79	9.3

Table II. Parameters of Spectra with First Harmonic Emission

Spectrum ^[a]	ν_L^0 (keV) ^[b]	ν_c (keV)	$T(kT_e/mc^2)$ ^[c]	$J(10^{12} \text{ gauss})$
9-16-78	40	11	.36	7.32
9-18-78 ¹	20	1.8	.23	2.93
10-12-78B	43	8.8	.32	7.27
11-09-78	35	4.1	.26	5.23
1-19-79	35	3.4	.24	5.09
2-13-79	28	5.3	.32	4.46
2-15-79	28	9.5	.39	5.38
3-13-79 ³	32	10	.38	5.97 [b]
3-13-79 ⁷	32	0.6	.12	3.59
3-29-79 ¹	18	10	.49	3.59 [b]
3-29-79 ⁸	18	0.032	.04	1.72
4-02-79B ³	32	13	.43	6.32
4-24-79A	18	2.7	.29	2.77
5-24-79	18	5.0	.37	3.15
5-26-79	50	3.8	.22	6.77
6-12-79	32	3.4	.25	4.69
6-28-79A	32	7.4	.34	5.52
7-05-79	32	1.6	.18	4.26
7-12-79	23	1.9	.22	3.38
10-07-79	18	3.3	.31	2.96
11-09-79 ²	30	1.8	.19	4.30
11-11-79 ³	30	2.5	.22	4.29
1-16-80	30	3.0	.24	4.45
1-26-80	40	1.4	.16	5.10

- [a] Superscripts above event date denote time interval of spectrum for events with reported spectral evolution (see Mazets et al. 1981).
- [b] ν_L^0 denotes the estimated peak of the observed emission feature. Since in most cases there is no data with energy below ν_L^0 , the actual first harmonic peak may lie slightly below the listed value. In that case the actual B would be slightly below, and the actual T would be slightly above the listed values. Because of these uncertainties, the apparent evolution of B-field for the 3-13-79 and 3-29-79 events should not be taken at face value.
- [c] $T = \sqrt{\nu_c \lambda_L^0 / \Gamma(T)}$ where the relativistic Doppler factor $\Gamma(T) \approx 1 + c_v T$ with $c_v \approx 3$ in the present temperature ranges (see numerical results in Lamb 1982). No allowance for gravitational redshifting (which could be as much as 20-30 percent) has been included in these T and B estimates.

Table III. Spectra with Possible First and SecondHarmonic Emission Features

Spectrum	1st Harmonic Location ν_1 (keV)	2nd Harmonic Location ν_2 (keV)	F ₁ /F ₂ Flux Ratio Observed	TS Prediction
9-16-78	40	80	1.25	1.32
10-12-78B	43	85	1.83	1.57
11-09-78	35	70	2.0	1.92
4-02-79B ³	32	65	1.32	1.16
4-24-79A	18	36	1.85	1.72
5-24-79	18	36	4.0	1.35
6-28-79A	32	65	1.36	1.47
7-05-79 ²	32	65	2.5	2.78

Note:

In some cases the emission features can in principle be viewed as cyclotron absorption features of lower field strength. But the excellent agreement between columns 4 and 5 in almost all cases suggests that the harmonic emission interpretation is likely correct.

Table IV. Spectra with Self-Absorption

Spectrum	ν_{ab}^{\dagger} (keV)	ν_c (keV)	$n_e h / TK_2(T^{-1})$ ($10^{22}/\text{cm}^2$)	Assuming $\nu_L^0 \leq \nu_{ab}$			
				$T \geq$	$\tau_{es}(10^{-4}) \geq$	$\frac{L_{syn} \geq}{A(\text{km}^2)}$	$\frac{d(\text{kpc})^* \geq}{A^{1/2}(\text{km})}$
10-06-78A	30	9.9	1.6	.39	2.2	4.5×10^{40}	30
11-04-78A	25	2.1	5.2	.22	.34	3.1×10^{39}	10
11-07-78	42	6.0	4.8	.29	1.7	3.3×10^{40}	37
11-11-78	28	1.9	7.7	.20	.24	3.2×10^{39}	11
11-19-78 ¹	40	110	0.6	.87	.20	4.9×10^{42}	38
11-19-78 ³	40	6.0	4.3	.29	1.5	3.0×10^{40}	10
11-21-78A	26	4.8	2.3	.31	1.2	1.1×10^{40}	19
2-14-79	30	4.1	3.5	.28	1.0	1.1×10^{40}	13
4-02-79B ¹	60	50	1.7	.56	9.7	1.7×10^{42}	49
4-06-79	45	38	1.2	.56	6.9	7.5×10^{41}	50
6-13-79	50	1.9	32.2	.17	.33	9.3×10^{41}	72
10-14-79 ¹	40	5.9	4.4	.28	1.1	2.8×10^{40}	15
11-11-79 ¹	50	5.9	6.9	.24	0.6	3.8×10^{40}	30

[†]The self-absorption frequency ν_{ab} is approximately where the optically thin spectrum would intersect the Rayleigh-Jeans part of the black-body spectrum.

*Due to anisotropy of the radiation pattern and unknown B-field orientation and other factors, these distance limits must be considered as uncertain by at least a factor of 2. Moreover, no gravitational redshifting has been included here, which would lower d by an additional $(1+z)^{-1/2}$.

ORIGINAL PAGE IS
OF POOR QUALITY

Table V. Comparison Between Parameters Determined by
TS, TB and IC Fits to the Spectrum of 9-18-78⁴

	TS ($\nu_c = 6.2$ keV)	TB	IC
	(assume $\nu_L^0 < 25$ keV)		
T	≥ 180 keV	317 keV	200 keV
	(assume $\nu_{ab} < 25$ keV)		
r_{es}	$\leq 3.5 \times 10^{-4}$	-	~ 1
	(assume $\nu_{ab} < 25$ keV)		
n_{eh}^2		$\leq 10^{54}$	

FIGURE CAPTIONS

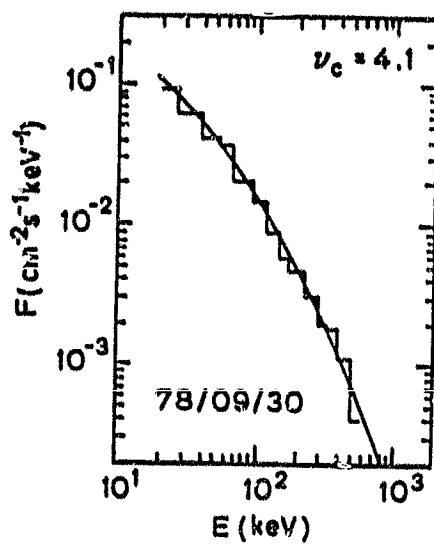
Figure 1 Representative gamma-burst spectra typical of the "perfect fits" with the thermal synchrotron model. Values of ν_c corresponding to the theory curves are listed in upper righthand corners.

Figure 2 Representative spectra with high-energy tail deficiencies compared to the theoretical TS curves.

Figure 3 Representative spectra with emission excesses above the TS curves in the 300-800 keV range. (a) and (b) are typical of "broad" features, while (d) is typical of the narrow "line" at ~ 400 keV, interpretable as the redshifted 511 keV line. (c) has the unique property that the feature was very broad at early times (spectrum 1, observation by U.S. groups, may have resolved it into two separate lines at 400 and 800 keV), but evolved into a narrow line at ~ 600 keV at later times (spectrum 3), which, if real, can correspond only to a blueshifted 511 keV line. The feature is not evident at time 2. Note that spectra 1 and 3, which have the emission feature, also show evidence of self-absorption at the low-energy end, probably corresponding to higher total electron (pair) column density due to the abundance of pairs.

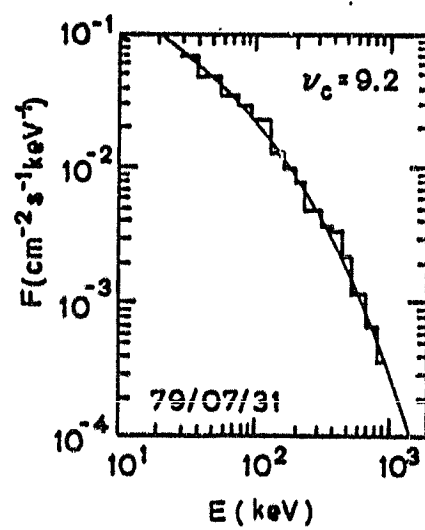
- Figure 4 Representative spectra exhibiting self-absorption. Dashed curves are possible Rayleigh-Jeans limits corresponding to the appropriate electron temperature.
- Figure 5 Representative spectra exhibiting first (or even the second) harmonic emissions at energies below the TS continuum. Dashed curves suggest possible profiles of the harmonics and are not detailed model fitting.
- Figure 6 Representative spectra with the controversial cyclotron absorption dips at 40-65 keV. Note that the TS fits continue to be excellent below the dips.
- Figure 7 Histogram of ν_c distribution according to the total number of published spectra (a) and events (b).
- Figure 8 Time evolution of ν_c for 14 events with reported spectral evolution.
- Figure 9 Histograms of T and B distributions for the 22 events with possible first harmonic emission features.
- Figure 10 Comparisons between TS, TB and IC fits to the continuum spectrum of 9-18-78.⁴ The narrow feature at 400 keV is removed from the fitting procedures.

ORIGINAL PAGE IS
OF POOR QUALITY



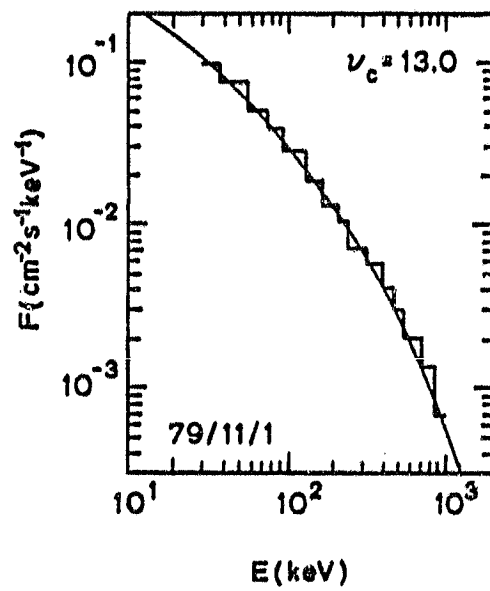
(1a)

ORIGINAL PAGE IS
OF POOR QUALITY



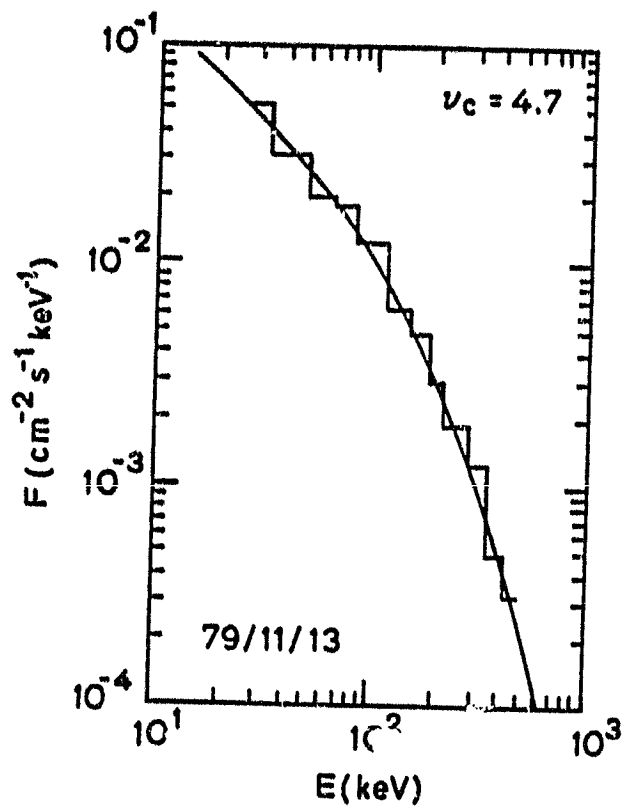
(1b)

ORIGINAL PAGE IS
OF POOR QUALITY



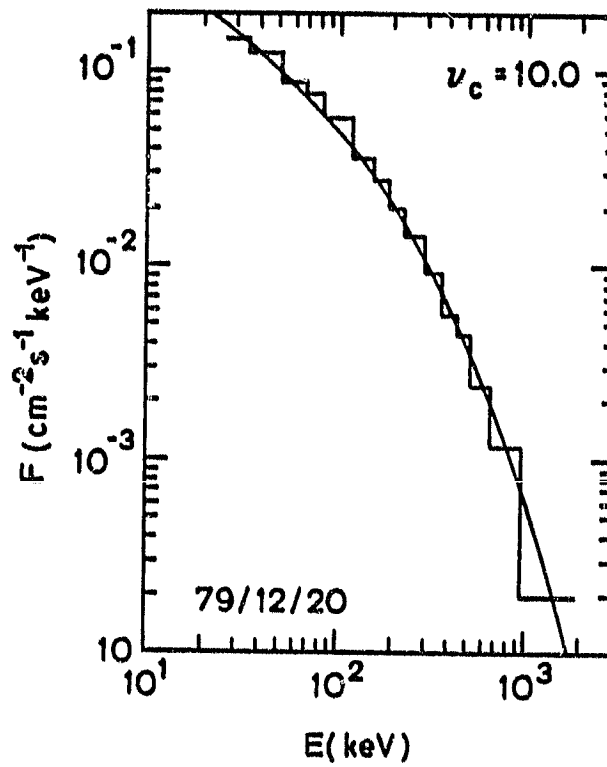
(1c)

ORIGINAL PAGE IS
OF POOR QUALITY



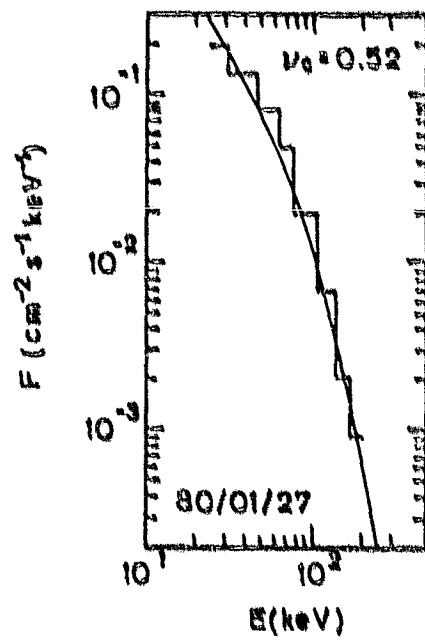
(1d)

ORIGINAL PAGE IS
OF POOR QUALITY



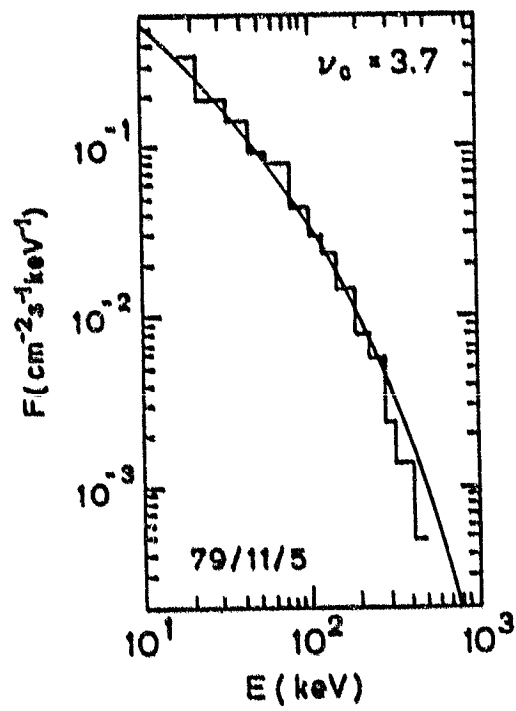
(1e)

ORIGINAL
OF POOR QUALITY



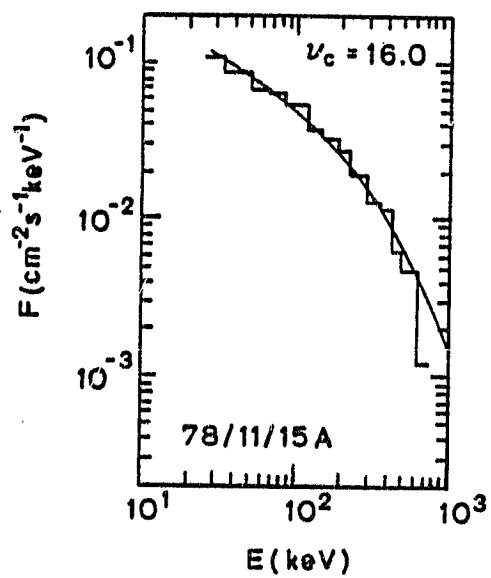
(1 f)

ORIGINAL PAGE IS
OF POOR QUALITY



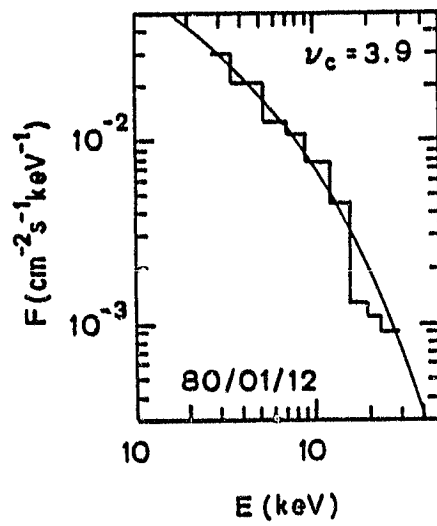
(2a)

ORIGINAL PAGE IS
OF POOR QUALITY



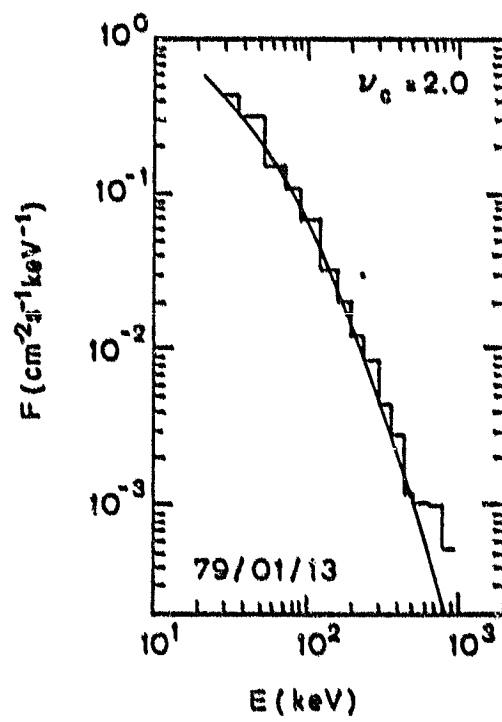
(2b)

ORIGINAL PAGE IS
OF POOR QUALITY



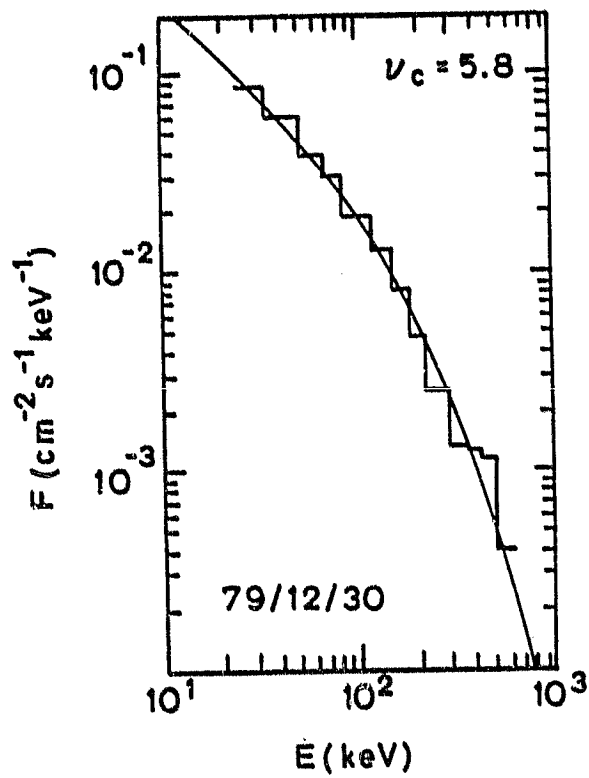
(2c)

ORIGINAL PAGE IS
OF POOR QUALITY



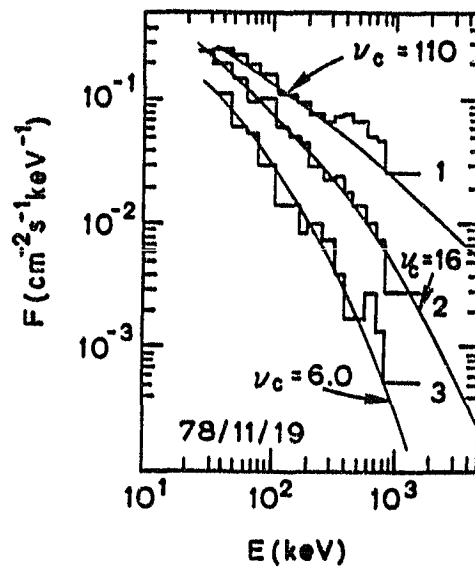
(3a)

ORIGINAL PAGE IS
OF POOR QUALITY



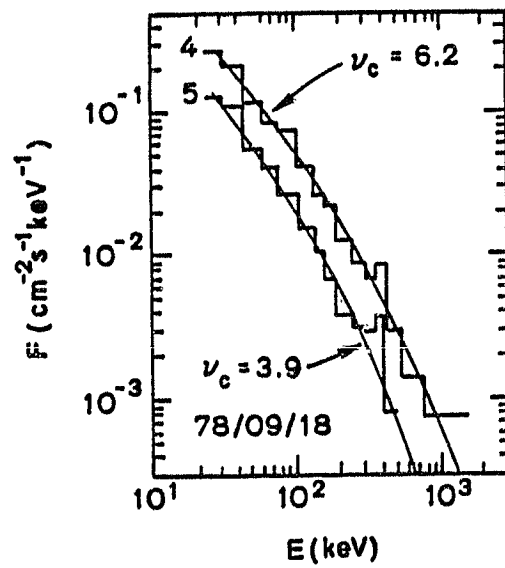
(3b)

ORIGINAL PAGE IS
OF POOR QUALITY



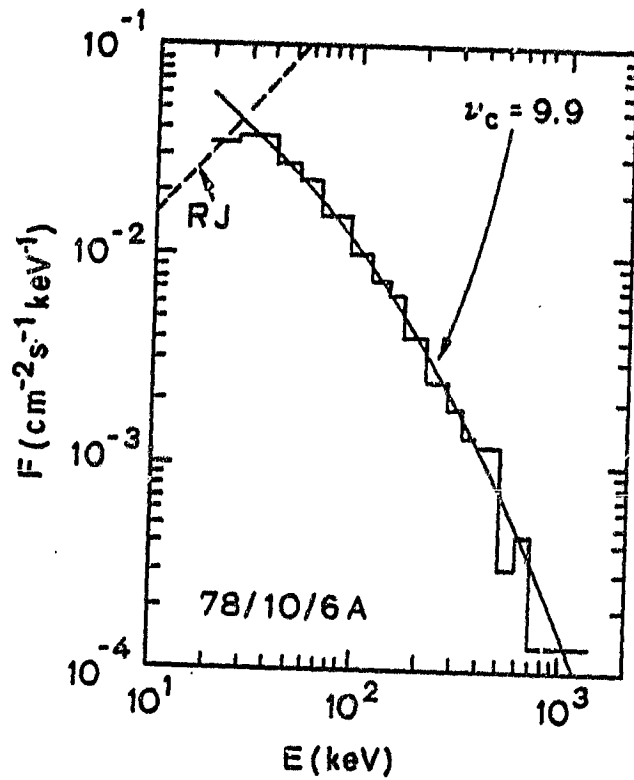
(3c)

ORIGINAL PAGE IS
OF POOR QUALITY



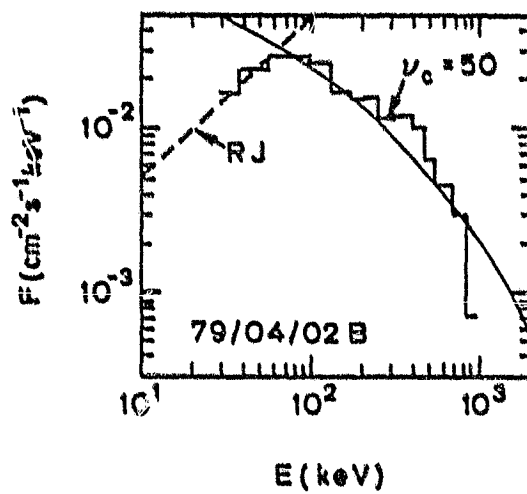
(3d)

ORIGINAL PAGE IS
OF POOR QUALITY



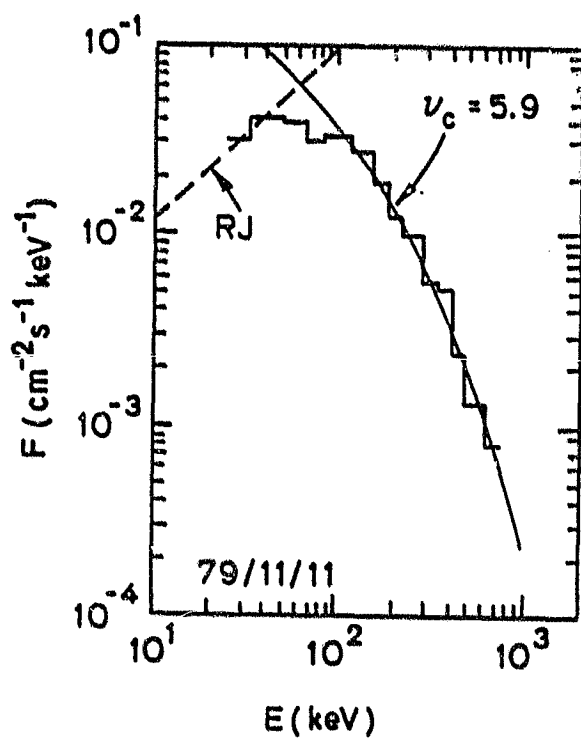
(4a)

ORIGINAL PAGE IS
OF POOR QUALITY



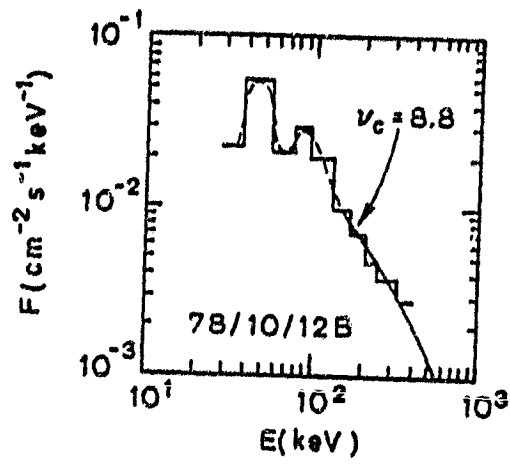
(4b)

ORIGINAL PAGE IS
OF POOR QUALITY



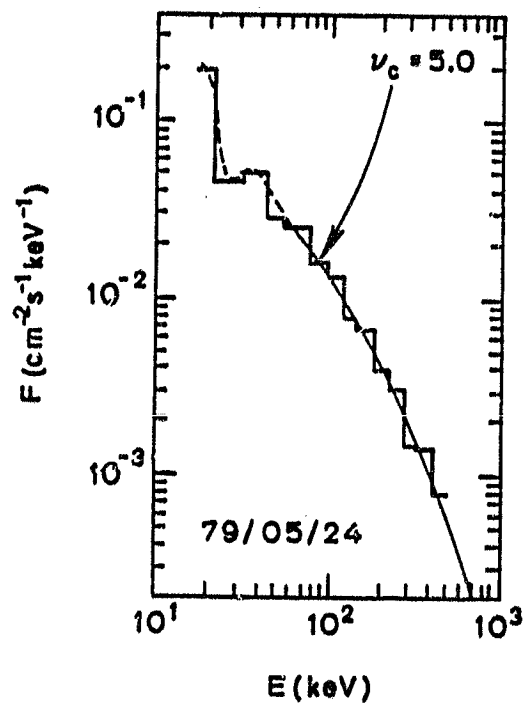
(4c)

ORIGINAL PAGE IS
OF POOR QUALITY



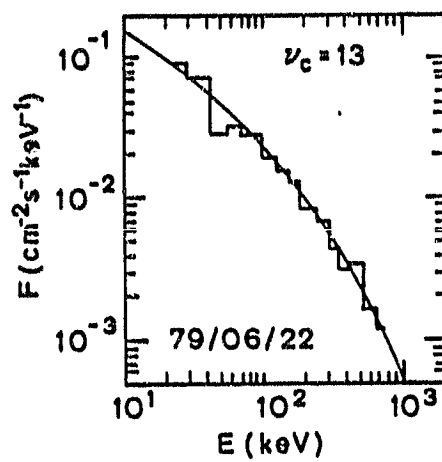
(5a)

ORIGINAL PAGE IS
OF POOR QUALITY



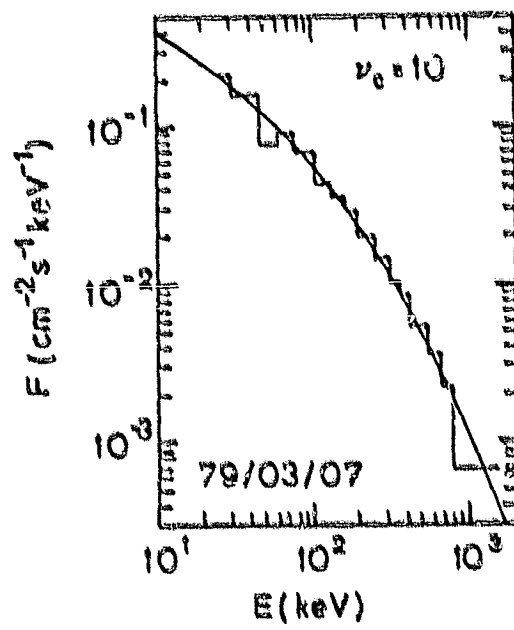
(5b)

ORIGINAL PAGE IS
OF POOR QUALITY.



(6a)

ORIGINAL PAGE IS
OF POOR QUALITY



(6b)

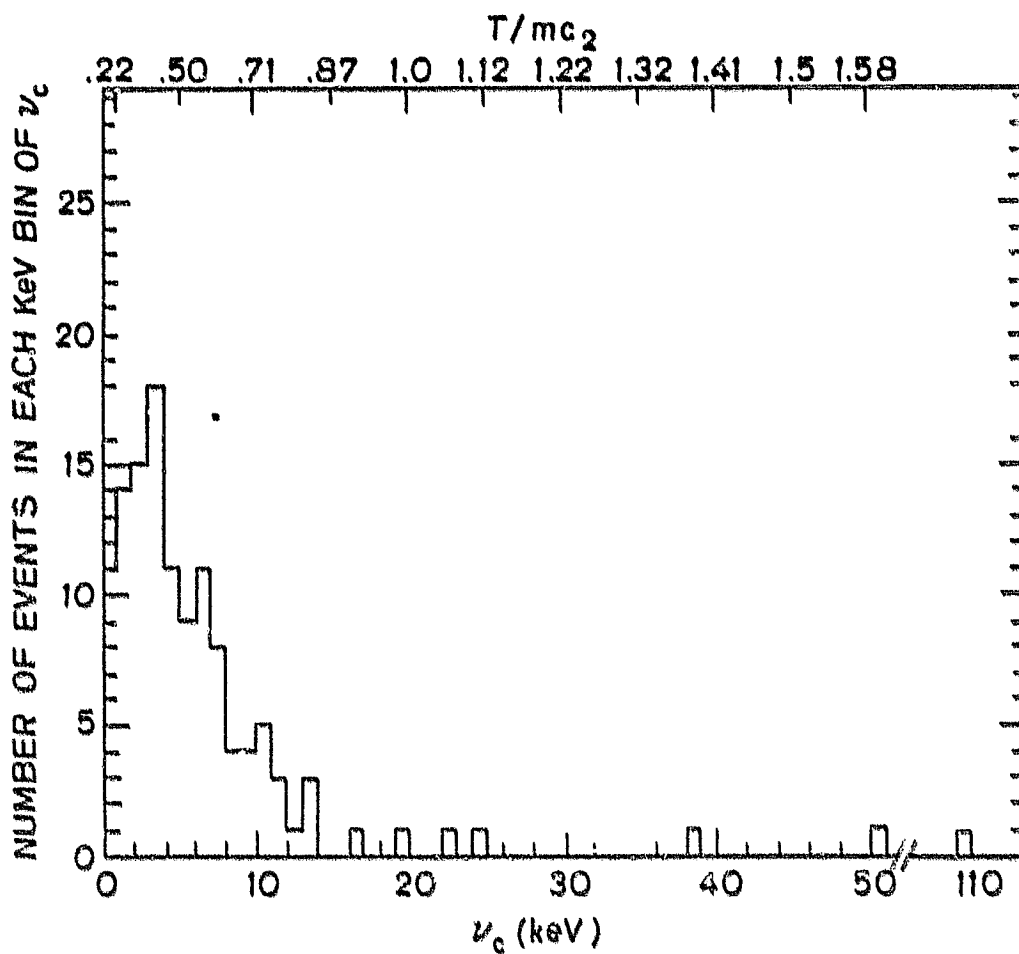
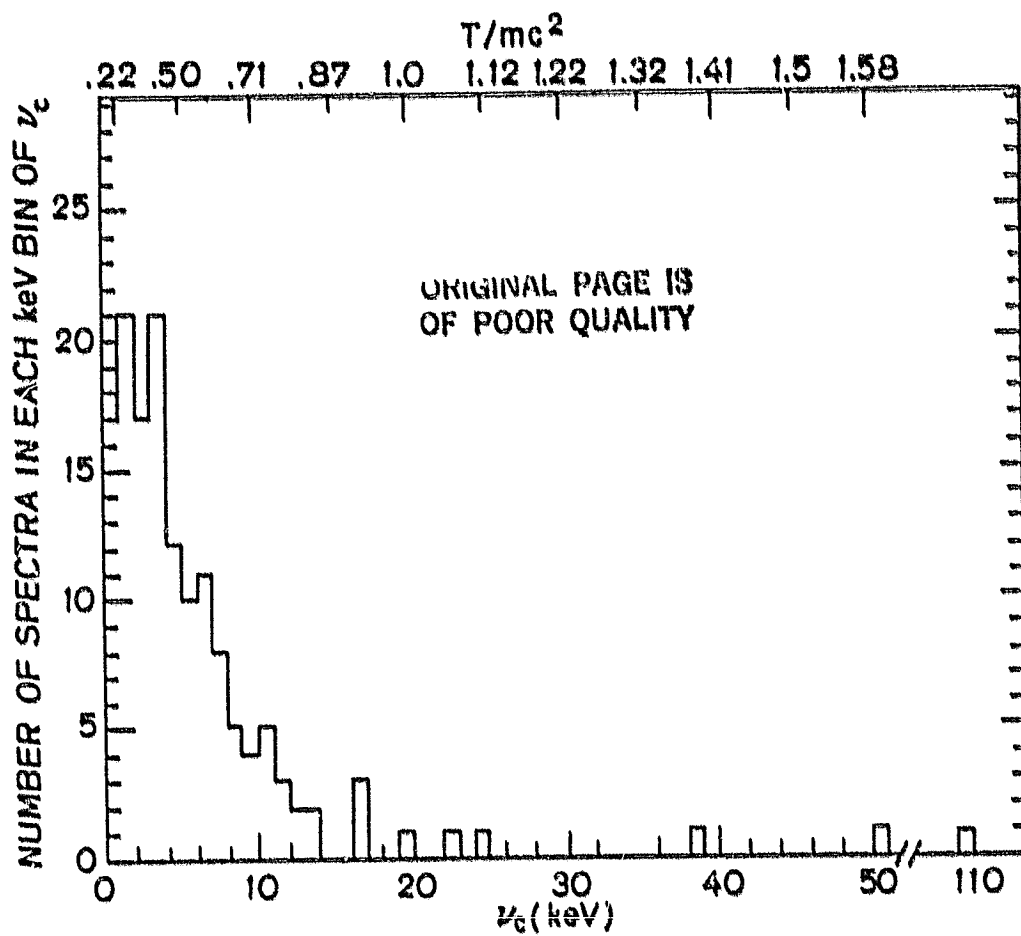


Figure 7

ORIGINAL PAGE IS
OF POOR QUALITY

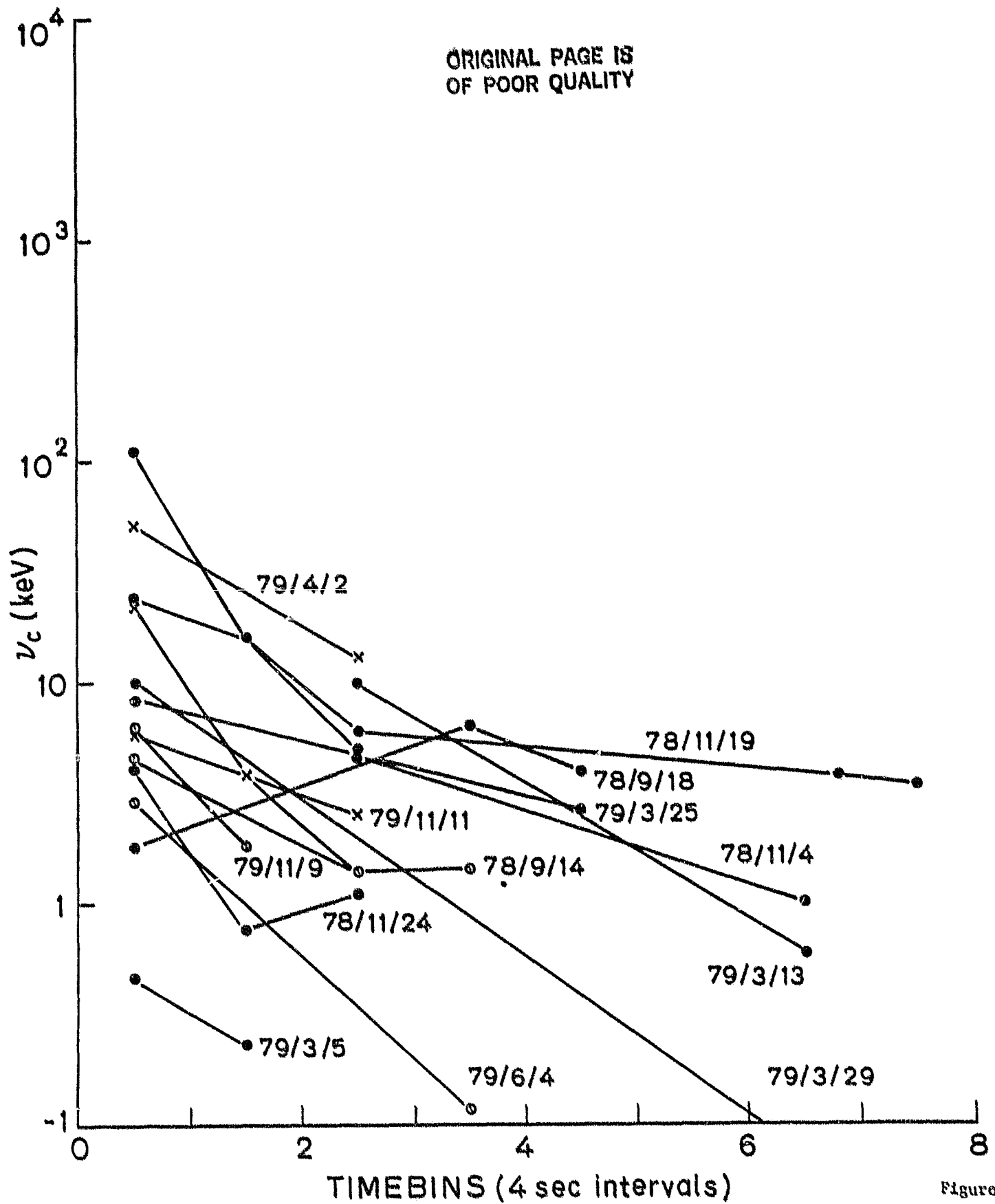


Figure 8

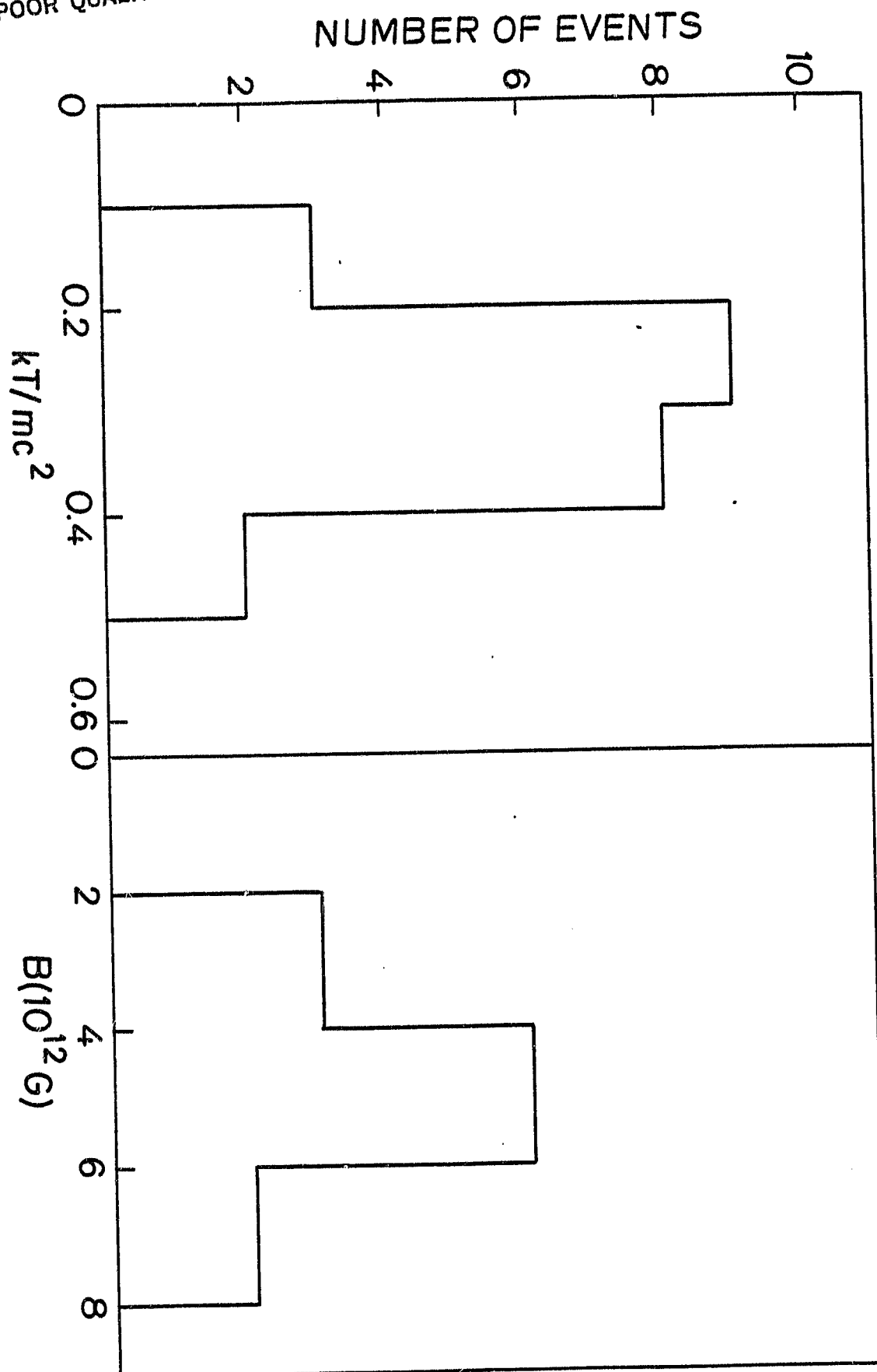


Figure 9

ORIGINAL PAGE IS
OF POOR QUALITY

9/18/78⁴

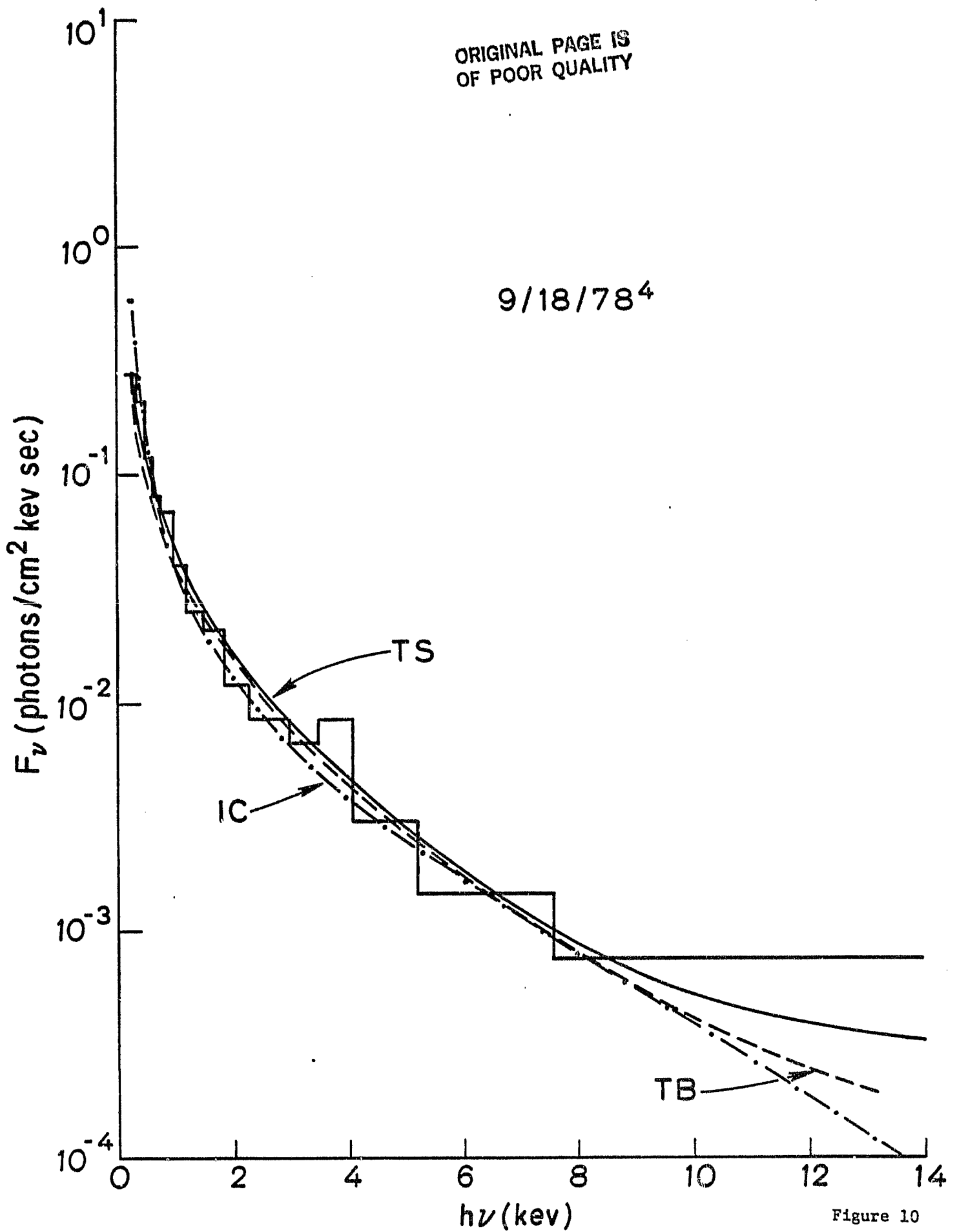


Figure 10